Cover Page

Universiteit Leiden

Author: Rosalia, Rodney Alexander
Title: Particulate based vaccines for cancer immunotherapy
Issue Date: 2014-10-02

Chapter 8

Targeting nanoparticles to CD40, DEC-205 or CD11c molecules on DC for efficient CD8$^+$ T cell responses; a comparative study

Luis J. Cruz*, Rodney A. Rosalia*, Jan Willem Kleinovink,
Felix Rueda, Clemens W.G.M. Löwik, Ferry Ossendorp

* Contributed equally to this study

Abstract

Here we demonstrate the importance of targeting antigens (Ags) to dendritic cell (DC) receptors to achieve an efficient cytotoxic T cell response which was associated with a strong activation of DC. Pegylated poly(lactic-co-glycolic acid) (PLGA) nanoparticles (NP), encapsulating Ovalbumin (OVA) as a model protein Ag and Toll like receptor (TLR) 3 and 7 ligands were targeted to distinct DC cell-surface molecules; CD40, a TNF-α family receptor, DEC205, a C-type lectin receptor or CD11c, an integrin receptor, by means of specific monoclonal antibodies (mAb) coupled to the NP. The efficiency of these different targeting strategies to activate DC and elicit a potent $CD8^+$ T cell response was studied. PLGA-(Ag/TLR3+7L) NP were more efficiently targeted to and internalized by DC *in vitro* compared to the control non-targeted NP. We observed a small but significantly improved internalization of CD40-targeted NP compared to DEC-205 or CD11c targeted NP. In contrast to non-targeted NP, all targeted NP equally stimulated IL-12 production and expression of co-stimulatory molecules by DC, inducing strong proliferation and IFN-y production by T cells *in vitro*. Upon subcutaneous (s.c.) vaccination CD40, DEC-205 and CD11c targeted NP consistently showed higher efficacy than non-targeted NP to stimulate $CD8^+$ T cell responses. However, all targeted NP vaccines showed equal capacity to prime $CD8^+$ T cells capable of target cell lysis *in vivo*. In conclusion, delivery of NP-vaccines to DC by targeting via cell-surface molecules leads to strong enhancement of vaccine potency and induction of T cell responses compared to non-specific delivery of NP to DC.

Introduction

The specificity, strength, and persistence of the immune response have led many research teams to focus their efforts on producing vaccines against various immunological diseases. It is well described that the immune system has the potential to recognize and eliminate cancerous cells [1-3]. The primary goal of cancer vaccination is the generation of robust and specific T cell responses with the capacity to inhibit tumor growth [4-6] in cancer patients with otherwise poor natural tumor specific immunity. In this respect, dendritic cells (DCs) have a crucial role as these cells are considered the most efficient and specialized Ag-presenting cells (APCs) with the capacity stimulate strong cytotoxic T cell responses by cross-presenting tumor-derived protein antigens. Vaccination strategies involving DCs have been studied owing to their function in coordinating innate and adaptive immune responses *in vivo* [7-9]. and given that DCs are stimuled appropriately they initiate and direct robust antitumor immune responses. DC-based therapies have shown some clinical benefits; however their use is hampered by laborious vaccine preparations requiring multiple and complex steps to adhere to good manufacturing practices (GMP)-regulations and donor variabilities.

The drawbacks of DC-based therapies can be circumvented by delivery of specific protein antigens (Ags) to DCs directly *in vivo* via specific surface receptors using for example poly-(lactic-co-glycolic-acid) (PLGA) particulate delivery systems. One of the greatest benefits of particle-based Ag delivery systems resides in their capacity to carry polypeptide Ags and adjuvants concomitly to the same APC, which was shown to efficiently induce T cell responses [10-13]. Furthermore, the targeted delivery of Ags to DC surface receptors enhances presentation to T cells [14]. However, it is not fully clear, which cell surface molecule or receptor expressed by DC should targeted for optimal T cell activation.

To address this issue, three distinct cell-surface receptors will be analyzed for the targeting and delivery of NP-based vaccines to DC: CD40, a TNF-α family receptor with known DC activating properties after binding of its specific ligand, DEC-205, a C-type lectin receptor, and integrin receptor CD11c which does not induce DC activation after binding of their respective ligands. In this work, Ovalbumin protein Ag will be encapsulated together with the Toll-like Receptor (TLR) ligands (TLRLs) polyinosinic:polycytidylic acid (poly I:C) (TLR3) and resiquimod (R848) (TLR7), two potent immunostimulatory agents that mimic pathogen-derived material and function by triggering endosomal TLRs.

NP delivery to DC by targeting the appropriate cell-surface receptor might further enhance the activation of DC by TLRLs, either via enhanced internalization of the TLRLs into the

8

endosomes or through triggering of cell-surface molecules with separate downstream DC-activating signaling pathways which possibly synergizes with TLR-stimulation.

Herein a comparative study of the responses induced by targeting these different DC receptors is presented. We show here the strong requirement for cell surface molecule targeting on DC to enhance internalization of NP by DC and enhance immune activation compared to non-targeted controls. However in our model, targeting CD40, DEC-205 or CD11c resulted in comparable immune responses. This is highlighted by observing similar rates of diffusion of all targeted NP out of the injection site, whereas non-targeted NP were significantly slower in this process. In addition, vaccination with the different targeted NP led to CD8^{+} T cell responses with similar proliferative potential, IFN-γ production and *in vivo* cytotoxicity against specific target cells.

Material and methods

Materials and reagents

PLGA (Resomer RG 502 H, lactide:glycolide molar ratio 48:52 to 52:48); MW: 7000-17000 Da was purchased from Boehringer Ingelheim, Germany. Solvents for peptide synthesis and PLGA preparation (dichloromethane (DCM), N,N'-dimethylformamide (DMF) and ethyl acetate) were obtained from Sigma-Adrich (The Netherlands). Lipids purchased from Avanti Polar Lipids (USA) include 1,2-distearoyl-sn-glycero-3-phosphoethanolamine-N-[succinic acid(polyethylene glycol)2000] (ammonium salt) and 1,2-distearoyl-sn-glycero-3-phosphoethanolamine-N-[methoxy(polyethylene glycol)-2000] (ammonium salt) (mPEG 2000 PE). R848 was from Axorra, poly I:C from Sigma and endotoxin free OVA from Hyglos GmbH.

Anti-CD40 mAb (clone FGK45, IgG2a) was produced in house after obtaining the hybridoma from A. Rolink (Basel Institute for Immunology, Basel, Switzerland) [15]. Mouse anti-CD11c and the murine anti-DEC205 (CD205) Abs were from BIO-X-CELL (West Lebanon, NH). Mouse IgG2a Isotype control (Clone:C1.18.4 Catalog #:BE0085) and mouse IgG2b Isotype control (Clone:MPC-11Catalog #:BE0086) were also purchased from Bio X Cell Antibody Production and Purification.

Preparation and characterization of PLGA NP

PLGA-NP coated with Abs was generated using the copolymer PLGA essentially as described before [16,17]. In brief, 100 mg of PLGA in 2 mL of ethyl acetate containing OVA Ag free endotoxin (10 mg) and/or poly I:C (4 mg) and/or R848 (1 mg) were emulsified under sonification (Branson, sonofier 250) during 60 seconds. This first emulsion was rapidly added to 1 mL of 1% polyvinylalcohol(PVA)/7% ethyl acetate in distillated water during 15 second. A combination of lipids (DSPE-PEG(2000) succinic acid (8 mg) and mPEG 2000 PE (8 mg)) were dissolved in chloroform and added to the vial. The chloroform was removed by a stream of nitrogen gas. Subsequently, the emulsion was rapidly added to the vial containing the lipids and the solution was homogenized during 30 seconds using a sonicator. This solution was added to 100 mL of 0.3% PVA 7% of ethyl acetate in distillated water and stirred overnight to evaporate ethyl acetate. The PLGA-NP were collected by centrifugation at 12000 x g for 10 min, washed four times with distilled water and lyophilized. Next, abs was covalently coupled to 10 mg of PLGA NP by activating surface carboxyl groups in isotonic 0.1 M MES buffer pH 5.5 containing 1-ethyl-3-[3-dimethylaminopropyl] carbodiimide hydrochloride (10 equiv.) and N-hydroxysuccinimide (10 equiv.) for 1 h. The activated carboxyl-PLGA NP was washed one time with MES buffer by centrifugation. Subsequently, abs (αCD40, αCD11c, αDEC-205 and isotype controls respectively (200 µg per mg NP) were added and the solution was stirred during 3 h at room temperature and later overnight at 4°C. Unbound antibodies were removed by centrifugation (12000 x g, during 10 min) and the PLGA NPs-Abs was washed four times with PBS. The presence of Abs on the particle surface was determined by Coomassie dye protein assay (Table 8.1).

Dynamic light scattering and zeta-potential measurements

Dynamic light scattering (DLS) measurements were taken on different PLGA-NP using an ALV light-scattering instrument equipped with an ALV5000/60X0 Multiple Tau Correlator and an Oxxius SLIM-532 150 mW DPSS laser operating at a wavelength of 532 nm. A refractive index matching bath of filtered cis-decalin surrounded the cylindrical scattering cell, and the temperature was controlled at 21.5 ± 0.3 °C using a Haake F3-K thermostat. In each sample, the g2(τ) auto-correlation function was recorded ten times at a detection angle of 90°. For each measurement, the diffusion coefficient (D) was determined by using the second-order cumulant, and the corresponding PLGA NP diameter was calculated

8

assuming that the PLGA NP were spherical in shape. Zeta potential measurements were performed on PLGA NP using a Malvern ZetaSizer 2000 (UK).

Quantifying encapsulated OVA in NP

OVA-protein encapsulating efficiency was determined after hydrolyzing 5 mg PLGA NP in 0.5 mL 0.8 M NaOH overnight at 37°C. The OVA-protein content was then measured using Coomassie Plus Protein Assay Reagent (Pierce) according to the manufacturer's protocol. OVA encapsulation efficiency was calculated by dividing the measured amount of encapsulated Ag by the theoretical amount assuming all was encapsulated.

Quantifying encapsulated TLR ligands

Biodegradable PLGA NP was hydrolyzed with 0.8 M NaOH overnight at 37°C. The encapsulation efficiency of TLR ligands was determined by high-performance liquid chromatograph (HPLC). HPLC analysis was performed at room temperature using a Shimadzu system (Shimadzu Corporation, Kyoto, Japan) equipped with a RP-C18 symmetry column (250 mm x 4.6 mm). The flow rate was fixed at 1 mL/min and detection was obtained by UV detection at 220 nm. A linear gradient of 0% to 100% of acetonitrile (0.036% TFA) in water containing (0.045% TFA) was used for the separation of R848 and Poly I:C. The peak of R848 was well separated from that of the Poly I:C in the established chromatographic condition. The retention times of the Poly I:C and R848 were approximately 20 and 26 min, respectively. The regression analysis was constructed by plotting the peak–area ratio of R848 or Poly I:C versus concentration (ug/mL). The calibration curves were linear within the range of 1 ug/mL to 10 ug/mL for R848 and 2.5 ug/mL to 100 ug/mL for Poly I:C. The correlation coefficient (R^2) were always greater than 0.99, indicating a good linearity.

Animals

WT C57BL/6 mice (CD45.2/Thy1.2; H-2^b) were obtained from Charles River Laboratories. Albino B6 (B6(Cg)-Tyrc-2J/J), Ly5.1/CD45.1 (C57BL/6 background), transgenic OT-I/Thy1.1/ CD45.2 (specific for the OVA$_{257-264}$ CTL epitope presented by H2-K^b,) and transgenic OT-II/ Ly5.1/CD45.1 mice (specific for the OVA$_{323-339}$ Th epitope presented by I-A^b) were bred in the specific pathogen-free animal facility of the Leiden University Medical Center. All animal experiments were approved by the animal experimental committee of Leiden University.

Cell lines

D1 cells, a GM-CSF dependent immature dendritic cell line derived from spleen of WT C57BL/6 (H-2b) mice were cultured as described previously [18]. Freshly isolated DC (BMDC) were cultured from mouse bone marrow (BM) cells by collecting femurs from WT C57BL/6 mice or CD40 KO mice and cultured as published previously by our group [18]. After 10 days of culture, large numbers of typical DC were obtained which were at least 90% positive for murine DC marker CD11c (data not shown). The weakly immunogenic and highly aggressive OVA-transfected B16 tumor cell line (B16-OVA), syngeneic to the C57BL/6 strain, was cultured as described [19].

Analysis of *in vitro* NP-association with DC

WT C57BL/6 or CD40 KO BMDC (100,000/well) were plated into a 96-well flat bottom plate and incubated for 1 h at either 4°C (binding analysis) or 37°C (uptake analysis and kinetic uptake) with titrated amounts of targeted or non-targeted (PLGA-CW800-Ag/TLR3+7L)-PEG-mAbs (DC40, DEC-205, CD11c, IgG2b and IgG2a) formulations labeled with the near infrared dye (near-IR dyes, CW800). Cells were washed four times to remove residual non-bound NP. Binding, uptake and kinetic uptake of PLGA NP by DC was determined based on near-IR fluorescence using odyssey scanning (LI-COR) at 800 nm. Data analyses were corrected for the number of amount of cells per measurement via co-staining with TO-PRO® (Invitrogen) at 700 nm.

Analysis of *in vivo* NP-uptake upon vaccination

Animals were vaccinated with the CD11c, DEC-205 and CD40-targeted or non-targeted (PLGA-Ag/TLR3+7L) NP formulations containing OVA-Alexa647 (Invitrogen) by subcutaneous injection into the right flank. *In vivo* NP-uptake by cells was analyzed 48 h after vaccination by sacrificing the animals and isolating the inguinal lymph nodes and spleens. Single cell suspensions were prepared and flow cytometry was used to determine the fluorescence intensity of OVA-Alexa647 in F4/80⁻CD11b⁺CD11c⁺ DC as a measure for NP-uptake. All fluorescent-mAb used for staining were purchased from BD Pharmingen. Flow cytometry analysis was performed using a LSRII flow cytometer (BD Pharmingen) and analyzed with FlowJo software (Treestar).

8

In vitro MHC class I and II-restricted Ag presentation and T cell priming

DC were incubated for 5 h with the various (PLGA-Ag/TLRL)-mAb formulations at the indicated concentrations of OVA-protein Ag encapsulated in NP. After Ag incubation, supernatant were harvested and cells were then further co-cultured for 72 h in the presence of OT-I and OT-II splenocytes to assess OVA-specific MHC class II and class I-restricted proliferation of naïve CD4+ T cells and CD8+ respectively. Cells were pulsed with [3H]-thymidine for the last 16 hours of culture. Samples were then counted on a TopCountTM microplate scintillation counter (Packard Instrument Co., Meridan, CT, USA). Stimulation index was used as a measure for proliferation and was calculated as the fold increase of [3H]-thymidine CPM over the CPM counts obtained with medium as negative control.

Analysis of cytokine production by DC or T cells using Enzyme-linked Immunosorbent Assay (ELISA)

DC (100,000/well) were plated into a 96-well round bottom plate and incubated for 24 h with titrated amounts of Ag. Supernatants were harvested and tested for IL-12 p70 (BD OptEIA™ MOUSE IL-12 Cat. Nr 555256), IL-2 (BD OptEIA™ MOUSE IL-2 Cat. Nr 555148), following manufacturer's instructions.

In vivo visualization of NP vaccines

Nanoparticles carrying OVA labeled with the near-infrared fluorescent dye CW800 were visualized using the IVIS Spectrum preclinical *in vivo* imaging system (PerkinElmer). The fluorescent signal at the injection site was measured in time by drawing a region of interest (ROI) around the injection site and quantifying the total radiant efficiency in the 840 nm emission filter, expressed in [p/s]/ [μW/cm^2]. The signal was corrected for the background signal based on an identical ROI at an irrelevant position of the mouse.

OT-I transfer and analysis of CD8+ T cell expansion

The spleen was taken of an OT-I mouse on a CD90.1 background, mashed on a 70 um cell strainer to create a single-cell suspension. Then the CD8-negative cells were depleted by the CD8+ enrichment kit from BD. These cells were injected intravenously in the tail vein of the mice, in 200 uL PBS.

The mice were sacrificed and the inguinal LNs and the spleen were taken and mashed on a 70 um cell strainer. The left and right inguinal LNs were pooled, as they are both vaccine-draining. The cells were then stained with 7-AAD and with fluorescently labeled antibodies against CD8b and CD90.1. The *in vivo* proliferation of the OT-I cells was analyzed by calculating the percentage of CD90.1$^+$ cells within the total CD8b$^+$ population, excluding all 7-AAD$^+$ (dead) cells from the analysis.

Vaccination and immunization schemes

Animals were vaccinated with the various targeted or non-targeted (PLGA-Ag/TLRL) NP formulations by subcutaneous (s.c.) injection into the right flank or in the tail base region. Vaccine potency and activation of CD8$^+$ T cells were studied by transferring purified CD8$^+$ T cells from OT-I mice 2 days after tail-base vaccinations with different NP formulations. Priming of *in vivo* cytotoxic CD8$^+$ T cells were assessed seven days after vaccination in the right-flank by transferring spleen cells prepared from congeneic Ly5.1 C57BL/6 animals which were pulsed with the SIINFEKL short peptide (OVA$_8$/specific target cells) or ASNENMETM short peptide (FLU9/non-specific target cells). The target cells were labeled with either 10 µM (OVA) or 0.5 µM (Flu) CFSE. The cells were mixed 1:1 and 10*10^6 total cells were injected intravenously (i.v.) into the vaccinated animals. 18 h post transfer of target cells, animals were sacrificed and single cell suspensions were prepared from isolated spleens. Injected target cells were distinguished by APC-conjugated rat anti-mouse CD45.1 mAb (BD pharmingen). *In vivo* cytotoxicity was determined by flow cytometry using the following formula: (1-[(CFSE-peak OVA/CFSE-peak FLU)$^{vaccinated\ animals}$ x (CFSE-peak OVA/CFSE-peak FLU)$^{non-vaccinated\ animals}$]) x 100%.

Statistical analysis

Graph Pad Prism software version 5 was used for statistical analysis. Two-way Analysis of Variance (ANOVA) tests were used to evaluate cytokine production by DC or T cells across different concentrations of PLGA-NP containing adjuvants. Two-way ANOVA was also used to analyse differences in *in vitro* binding/uptake studies measuring NIR fluorescence. The differences in OVA-Alexa647 fluorescence upon *in vivo* uptake by immune cells were analyzed using the two-tailed unpaired Student *t* test or Mann Whitney test. Dose-response *in vitro* studies were analyzed using two-way ANOVA with Bonferroni posttests.

8

RESULTS

Design, preparation and characterization of PLGA NP

PLGA NP vaccines were generated using the biodegradable polymer PLGA. Figure 8.1 shows a schematic diagram of the targeted NP vaccine. The PLGA NP surface was coated with a polyethylene glycol (PEG)-lipid layer to minimize non-specific binding to cells other than DCs and to allow the incorporation of distinct DC receptors-specific Abs to effectively target mouse DCs. The morphology of PLGA NP was determined by transmission electron microscopy (TEM). Figure 8.1 shows a representative picture where the PLGA NP were uniform in size and showed spherical shape. TEM imaging clearly shows the presence of the PEG-lipid layer on the PLGA NP.

The characteristics of targeted PLGA NP containing fluorescent OVA Ag and TLR ligands (size distribution, polydispersity index, zeta potential, fluorescent Ag entrapment efficiency and amount of Abs conjugated to PLGA NP surface) are shown in Table 8.1. The encapsulation efficiency of fluorescent OVA Ag and TLRLs within the PLGA NP was determined by fluorescence assay and reverse phase high performance liquid chromatography respectively (Table 8.1). Exploiting dynamic light scattering (DLS) we found that the size of PLGA NP harboring fluorescent OVA with TLR ligands varied from 192.1 ± 11.3 nm and 246.0 ± 16.1 nm. It should be noted that the conjugation of Abs to
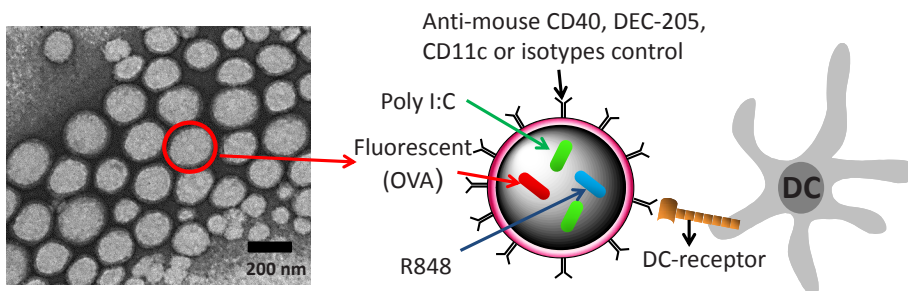

Figure 8.1   Schematic diagram of PLGA NP vaccines targeting DC-specific receptor on mouse DCs and PLGA NP analysis by TEM.
NP vaccines were generated carrying fluorescent OVA in combination with the TLR3 ligand poly I:C and the TLR7/8 ligand R848. Carriers were coated with a lipid-PEG layer to which distinct Abs (αCD40, αDEC-205, αCD11c and isotypes) were covalently attached on the PLGA NP surface. TEM image of a representative PLGA preparation. Image analysis revealed the presence of the PEG-lipid layer surrounding the NP. (Scale bar, 200 nm; magnification, 25000 x).

the PLGA NP alters the size. The hydrodynamic diameter of the PLGA NP increases when the Abs were incorporated on the PLGA NP surface. In addition, the zeta potential of Ab-coated PLGA NP was considerably less negative than the PLGA NP without Abs (Table 8.1). This reduction in the zeta potential reflects the conjugation reaction between the carboxyl group of PLGA NP and the amino groups of the Abs, providing additional evidence that the Abs were present on the PLGA NP surface. The amount of Abs present on the PLGA NP surface was in the range of 29.1 ± 3.1 µg to 37.0 ± 2.5 µg per mg PLGA, as determined by a Coomassie-based protein assay (see Table 8.1). All PLGA NP showed a relatively uniform size distribution, which was reflected by low polydispersity indexes (below to 0.234).

Analysis of PLGA NP binding and uptake by DC *in vitro*

DCs from wild type C57BL/6 mice were incubated with different amounts of PLGA NP (CW800-Ag/TLR3+7L)- targeted to CD40, DEC205 and CD11c receptors and isotype control (non-targeted) respectively at 4°C to determine their binding capacity towards DCs (Figure 8.2A). Fluorescence intensity was measured by Odyssey scanning as the ratio of PLGA NP containing CW800-OVA at 800 nm and the number of cell amount determined by nuclei staining at 700 nm. The ratio value indicates the level of binding of PLGA NP to the DC. A direct relation between the PLGA NP concentration and binding capacity was observed. Targeted PLGA NP showed statistically significant differences with respect to their non-targeted counterparts, being PLGA NP targeted to CD40 which presented the greatest binding capacity to the DC (Figure 8.2A).

Similar behavior was observed when the assay was performed at 37°C to analyze the uptake of PLGA NP by DCs (Figure 8.2B). Again, all the targeted PLGA NP showed statistically significant differences with respect to non-targeted NP and a direct relation among uptake and NP concentration was observed (Figure 8.2B). Additionally, when the kinetics of NP uptake by DC were studied over a 24 h period (Supporting Information Figure S8.1) a significant difference in the uptake of targeted PLGA NP was observed with respect to non-targeted PLGA NP.

Activation of DCs *in vitro* by targeted PLGA NP

The expression of CD40 and CD86, co-stimulatory molecules associated with DC-maturation, was studied by flow cytometry (Figure 8.3A). Almost the whole (> 90%) population of DCs was CD40+CD86+ double positive when PLGA NP were targeted to CD40, DEC205 and CD11c with respect to the their non-targeted counterparts or soluble

8

Table 8.1   Physicochemical characterization of targeted and non-targeted PLGA NP, size distribution and zeta potential

Samples	Poly I:C (μg/mg NP) (w/w) R848 (μg/mg NP) (w/w)	Antigen (μg/mg NP) (w/w)	PLGA NP diameter ± S.D. (nm)	Polydispersity index ± S.D.	Zeta potential ± S.D. (mV)	mAbs (μg/mg PLGA NP)
PLGA NP(OVA + Poly I:C + R848)-Non-mAbs	22 2.5	50	186.6 ± 09.0	0.086 ± 0.012	-34.4 ± 6.2	---
PLGA NP(OVA + Poly I:C + R848)-αCD40	22 2.5	50	200.7 ± 12.5	0.109 ± 0.025	-30.8 ± 2.3	29.1 ± 3.1
PLGA NP(OVA + Poly I:C + R848)-αDEC-205	22 2.5	50	198.2 ± 12.9	0.085 ± 0.016	-28.8 ± 2.5	32.0 ± 3.2
PLGA NP(OVA + Poly I:C + R848)-αCD11c	22 2.5	50	194.7 ± 11.6	0.148 ± 0.068	-30.0 ± 4.6	25.0 ± 3.7
PLGA NP(OVA + Poly I:C + R848)-Isotype (IgG2a)	22 2.5	50	192.1 ± 11.3	0.097 ± 0.046	-26.2 ± 2.5	34.0 ± 2.4
PLGA NP(OVA + Poly I:C + R848)-Isotype (IgG2b)	22 2.5	50	195.4 ± 14.3	0.122 ± 0.049	-31.0 ± 4.6	29.0 ± 3.2
PLGA NP(CW800-OVA + Poly I:C + R848)-Non-mAbs	12 2	25	204.8 ± 10.1	0.099 ± 0.016	-36.3 ± 1.6	---
PLGA NP(CW800-OVA + Poly I:C + R848)-αCD40	12 2	25	242.3 ± 25.0	0.167 ± 0.031	-30.4 ± 2.4	32.0 ± 2.2
PLGA NP(CW800-OVA + Poly I:C + R848)-αDEC-205	12 2	25	212.2 ± 10.4	0.121 ± 0.027	-31.4 ± 2.3	28.2 ± 3.2

PLGA NP(CW800-OVA + Poly I:C + R848)-αCD11c	12	2	219.8 ± 11.1	0.114 ± 0.022	-32.2 ± 2.8	31.3 ± 1.8
PLGA NP(CW800-OVA + Poly I:C + R848)-Isotype (IgG2a)	12	2	239.0 ± 13.6	0.234 ± 0.072	-29.6 ± 1.8	30.4 ± 1.4
PLGA NP(CW800-OVA + Poly I:C + R848)-Isotype (IgG2b)	12	2	232 ± 14.2	0.194 ± 0.058	-27.0 ± 2.4	32.0 ± 1.4
PLGA NP(Alexa-647-OVA + Poly I:C + R848)- Non-mAbs	20	2	202.5 ± 11.4	0.094 ± 0.042	-29.0 ± 2.4	---
PLGA NP(Alexa-647-OVA + Poly I:C + R848)- αCD40	20	2	216.0 ± 11.2	0.080 ± 0.032	-23.2 ± 2.9	35.0 ± 3.1
PLGA NP(Alexa-647-OVA + Poly I:C + R848)- αDEC-205	20	2	218.2 ± 13.4	0.074 ± 0.042	-24.5 ± 1.8	31.0 ± 2.3
PLGA NP(Alexa-647-OVA + Poly I:C + R848)- αCD11c	20	2	214.6 ± 14.1	0.064 ± 0.032	-22.5 ± 2.5	36.0 ± 2.5
PLGA NP(Alexa-647-OVA + Poly I:C + R848)- Isotype (IgG2a)	20	2	216.8 ± 16.1	0.074 ± 0.022	-26.5 ± 2.4	37.0 ± 2.5
PLGA NP(Alexa-647-OVA + Poly I:C + R848)- Isotype (IgG2b)	20	2	218.6 ± 10.1	0.084 ± 0.024	-23.5 ± 1.8	32.0 ± 2.4

PLGA NPs were characterized by DLS measurements and zeta potential measurements. PLGA NPs size data represent the mean value ± SD of ten readings from dynamic light scattering measurements. Zeta potential data represent the mean value ± SD of five readings. The encapsulation efficiency of TLR ligands (μg Poly I:C or R848 per mg NP) was determined by HPLC. The amount of antigens encapsulated inside of PLGA NPs (μg antigen per mg NP) was determined by Coomassie dye protein assay. The amount of antibody introduced into the PLGA NPs was determined indirectly by Coomassie Plus Protein Assay Reagent by measuring a small aliquot from the antibody solution at the starting point and at the end of the reaction.
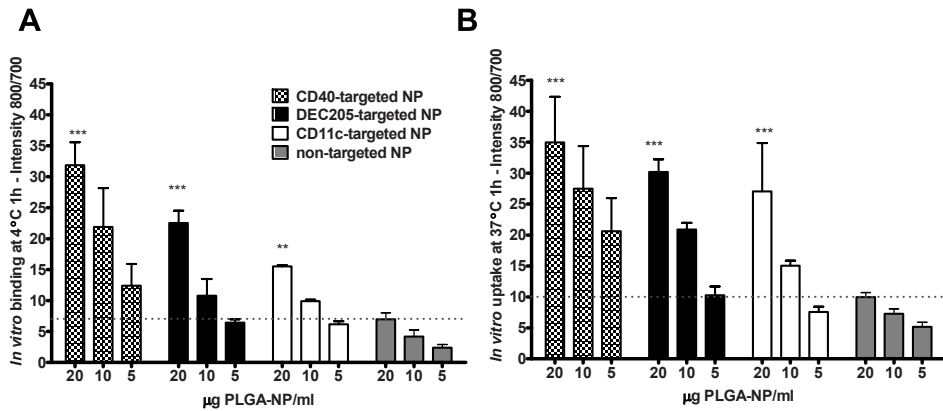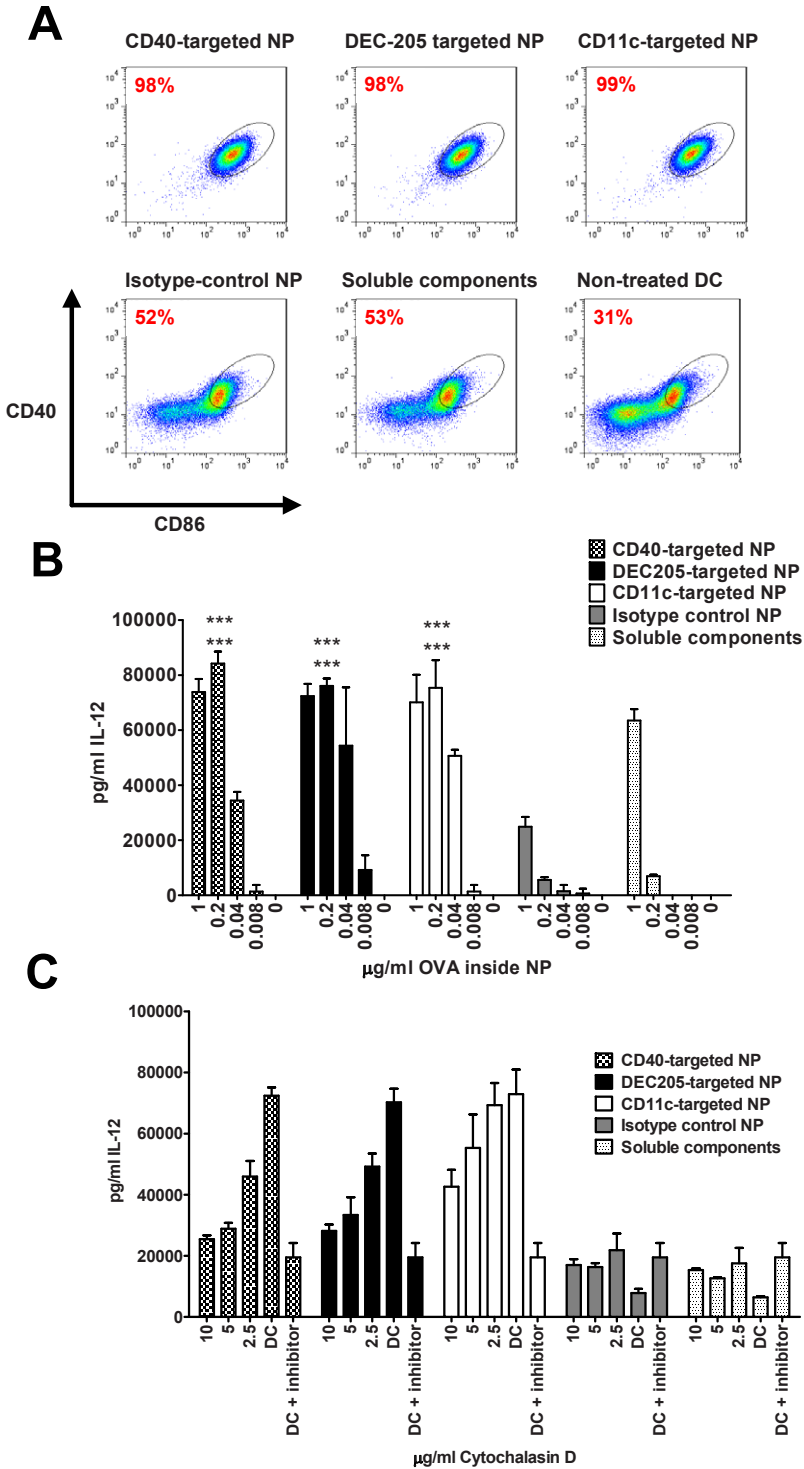
8

Figure 8.2 Targeting PLGA NP to DC facilitates binding and internalization compared to non-targeted NP.

WT C57BL/6 BMDC (100000 cells/well) were incubated with titrated amounts of PLGA-(Ag/TLR3+7L)-αCD40, PLGA-(Ag/TLR3+7L)-αDEC-205 and PLGA-(Ag/TLR3+7L)-αCD11c NP or isotype control (PLGA-(Ag/TLR3+7L)-non-targeted(pool of IgG2a and IgG2b bound PLGA-(Ag/TLR3+7) NP NP-formulations for 1 h at 4°C (A) or 37°C (B). Following washing (at least four time) to remove unbound NP, cells were co-staining with DNA-binding TO-PRO®, allowing quantification of number of cells per well and correlate with PLGA NP-binding or uptake per cells. Fluorescence intensity was measured by scanning on the Odyssey (LI-COR) and results shown the ratio of 800/700 nm fluorescence intensities of a duplicate analysis + deviation. Data are from one out of two independent experiments performed with two different batches of PLGA NP. Differences in PLGA NP-binding and uptake were analyzed applying two-way ANOVA with Bonferroni posttests, * = $P < 0.05$, ** = $P < 0.01$ and *** = $P < 0.0001$.

Figure 8.3 Improved maturation of targeted DC receptors by PLGA-(Ag/TLR3+7L) NP compared to PLGA-(Ag/TLR3+7L)-Isotype NP.

C57BL/6 BMDC (100000 cells/well) were incubated with titrated amounts of PLGA-(Ag/TLR3+7L) NP, either targeted or not, for 24 h at 37°C. Culture supernatants were harvested and the amount of IL-12 determined by ELISA **(A and B)**. Differences in cytokine production were analyzed applying two way ANOVA with Bonferroni posttests, * = $P < 0.05$, ** = $P < 0.01$ and *** = $P < 0.0001$. Data shown are mean ± SD from one representative experiment out of 3 independent experiments. **(C)** D1 dendritic cells (C57BL/6 background) were pre-incubated for 1 hr at 37°C with titrated amounts of cytochalasin D followed by a 24 h incubation with PLGA-(Ag/TLR3+7L) NP (based on 0.2 µg/mL encapsulated OVA), either targeted to CD40, DEC-205 and CD11c or non-targeted. Indicated amounts of cytochalasin D were maintained during the 24 h incubation with NP. After incubation, culture supernatants were harvested and analyzed for IL-12 amounts by ELISA as described in *Material and methods*.

A

CD40-targeted NP | DEC-205 targeted NP | CD11c-targeted NP

98% | 98% | 99%

Isotype-control NP | Soluble components | Non-treated DC

52% | 53% | 31%

CD40

CD86

B

Legend:
- ▨ CD40-targeted NP
- ■ DEC205-targeted NP
- □ CD11c-targeted NP
- ▨ Isotype control NP
- ▨ Soluble components

pg/ml IL-12

*** / ***

µg/ml OVA inside NP

C

Legend:
- ▨ CD40-targeted NP
- ■ DEC205-targeted NP
- □ CD11c-targeted NP
- ▨ Isotype control NP
- ▨ Soluble components

pg/ml IL-12

µg/ml Cytochalasin D

8

compounds which resulted in 50% or 30% CD40$^+$CD86$^+$ double positive cells, respectively (Figure 8.3A).

The *in vitro* production of IL-12 was also determined; DC loaded with PLGA NP targeted to the different receptors (namely CD40, DEC205 and CD11c) showed better IL-12 production with respect to the controls (Figure 8.3B). However, no activation differences were observed between the distinct formulations of targeted PLGA NP assayed for the above-mentioned receptors. Furthermore, it seems that an activation threshold exists with respect to the PLGA NP content. Thus, no differences were observed at the two highest amounts of NP used, indicated by 1 and 0.2 μg/mL of OVA, in contrast with the sharp drop observed when < 0.2 μg or lower were tested (Figure 8.3B). A lower production of IL-12 was observed using the isotype control NP and the soluble components (OVA, Poly I:C and R848 mixed) at all concentrations tested (Figure 8.3B).

Dendritic cells treated with titrated concentrations of Cytochalasin D, an inhibitor of actin polymerization which disrupts actin microfilaments associated with phagocytic uptake of exogenous material, showed a marked reduction of IL-12 production when cultured in the presence of targeted NP (Figure 8.3C). However, treatment with Cytochalasin D did not reduce the IL-12 production of DC cultured with non-targeted NP or soluble TLRLs (Figure 8.3C) (not shown).

T cell activation induced *in vitro* by PLGA NP containing Ag and TLR ligands targeted to specific DCs receptors

DC treated with the different PLGA-NP vaccines were used as APCs in co-cultures with splenocytes from OT-I mice (Figure 8.4A and C) or OT-II mice (Figure 8.4B and D) to determine the CD8$^+$ and CD4$^+$ T cell proliferation and IFN-γ production.

T cell proliferation (expressed as T cell stimulation index) of both CD8$^+$ and CD4$^+$ cells were efficiently induced by DCs loaded with targeted NP but not by the non-targeted counterparts (Figure 8.4A and B). However, no significant differences in the induction of T cell proliferation were observed between DCs loaded with the different targeted NP vaccines.

Similar observations were made analyzing IFN-γ amounts in culture supernatants after 48 h of culture (Figure 8.4C and D). Noteworthy was the sharp drop in IFN-γ amounts for all targeted formulations when < 0.2 μg/mL of OVA encapsulated in NP was tested (Figure 8.4C and D).
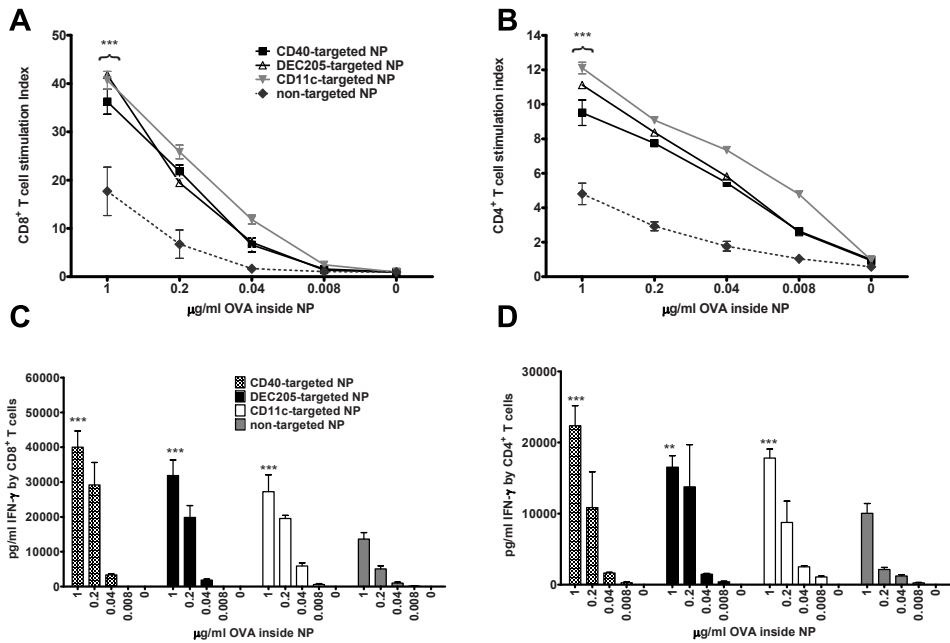
Figure 8.4   DCs loaded with CD40, DEC-205 or CD11C targeted NP containing OVA and TLR7 and 3 agonists show improved T cell stimulatory capacity compared to non-targeted controls. BMDC from C57BL/6 were incubated for 5 h at 37°C with titrated amounts of PLGA-(Ag/TLR3+7L) NP, either targeted to CD40, DEC-205 and CD11c or non-targeted. After incubation with Ag, 75% of the culture medium was removed and splenocytes (20,0000 splenocytes/well in a final volume of 200 μL/well) from OT-I **(A)** or OT-II **(B)** mice were added. OVA-specific T cell proliferation was measured 72 h later by analysis of [^{3}H]-thymidine incorporation which was added the last 16 hours of culture. Culture supernatants taken after 48 h of co-culture between Ag-loaded DC and OT-I or OT-II splenocytes were analyzed for IFN-γ levels **(C and D)**. Differences compared to non-targeted in T cell proliferation and cytokine production at the different conditions were analyzed applying two way ANOVA with Bonferroni posttests, * = P < 0.05, ** = P < 0.01 and *** = P < 0.0001. Data shown are mean ± SEM of two independent experiments.

8

Vaccination of C57BL/6 mice with PLGA NP targeted to CD40, DEC-205 or CD11c receptors

Vaccination with non-targeted or CD11c, DEC-205 or CD40 targeted NP (PLGA-Ag/TLR3+7L) containing TLR3 and 7 agonists and CW800-fluorescent labeled OVA as Ag were performed by subcutaneous injection into the tail base. At the indicated time points over a period
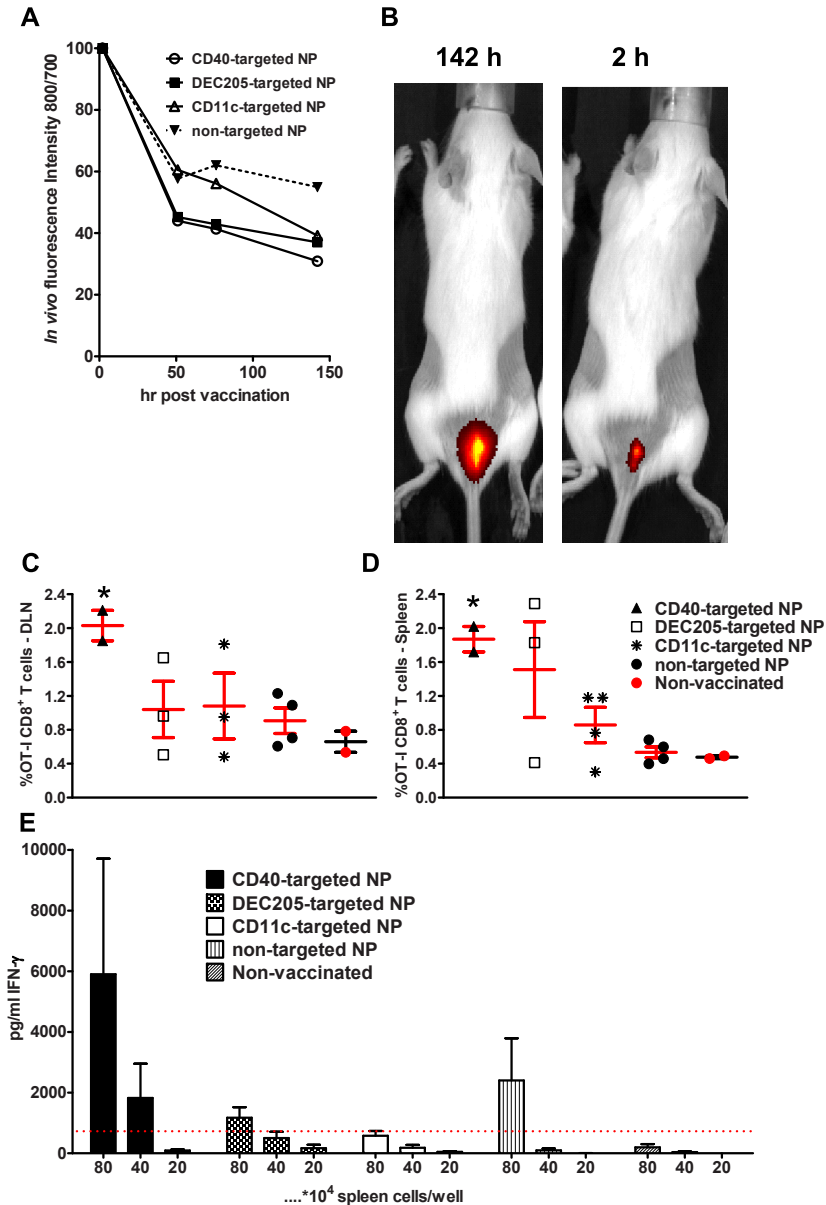
Figure 8.5   Facilitated transport out of the vaccination site results in better priming of CD8^{+} T cells by targeted PLGA NP.

Albino B6 mice were vaccinated s.c. in the tail-base region with 500 µg of PLGA NP containing CW800 fluorescent dye labeled OVA. PLGA NP were targeted to CD40, DEC-205 and CD11c or non-targeted. At designated time points animals were anesthetized. Live imaging of the vaccination site was performed to determine the outflow of particles in time **(A)** and graphically quantified as fluorescence intensity **(B).** 48 h after vaccination, mice received 1·10[6] purified OT-I CD8^{+} T cells. 4 days

of 6 days (Figure 8.5A) animals were anesthetized and live imaging of the fluorescence intensity at the injection site was carried out to determine the outflow of NP in time. The fluorescent signal declined over the first 24 h to 40–60% for all the formulations, whether targeted or not. The fluorescent signal progressively decreased during the next five days by 70%, except for the non-targeted formulation which remained at 40% (Figure 8.5B).

To determine the T cell activation induced by the targeted and non-targeted PLGA NP, 48 h after vaccination, mice received $1*10^6$ purified OT-I CD8$^+$ T cells. Four days later mice were sacrificed and the expansion specific of CD8$^+$ T cells in the draining inguinal lymph nodes (Figure 8.5C) and spleens (Figure 8.5D) was quantified by flow cytometry. CD40 targeted PLGA NP were most efficient in inducing T cell activation and expansion (Figure 8.5C and D).

Spleen cells from vaccinated animals were re-stimulated *ex vivo* with an OVA SIINFEKL-short peptide for 72 h and the production of IFN-γ was quantified in the culture supernatant (Figure 8.5E). A trend was observed that the CD40 targeted PLGA NP improved cytokine production after peptide stimulation compared to DEC205 and CD11c targeted PLGA NP but due to the high variability the differences were not statistically different (Figure 8.5E).

Vaccination of wild type mice with CD40, DEC-205 or CD11c-targeted PLGA-(Ag/TLR3+7L)-NP induces CD8$^+$ T cells with potent cytotoxic capacity *in vivo*

C57BL/6 mice were vaccinated s.c. in the right flank with 10 μg OVA encapsulated in CD40, DEC-205 or CD11c-targeted PLGA-(Ag/TLR3+7L) NP or non-targeted PLGA-(Ag/TLR3+7L) NP as a control. On day 7 post vaccination, target cells were labeled differentially with the CFSE label, pulsed with SIINFEKL short peptide (OVA$_8$/specific target cells) and negative control peptide as described in materials and methods. Cytotoxic activity induced by vaccination with PLGA NP targeted to DCs receptors was determined 18 h post transfer of these CFSE-Ag loaded target cells by flow cytometric analysis of single cell suspensions prepared from

8

later after CD8$^+$ T cell transfer mice were sacrificed and the % of OT-I cells from total CD8$^+$ T cells was analyzed in the DLN **(C)** and spleen **(D)**. Titrated amounts of spleen cells from vaccinated animals were stimulated with SIINFEKL-peptide for 72 h and the amount of IFN-γ in culture supernatants determined by ELISA **(E)**. Differences in fluorescence intensity were determined using student t tests (144 h post vaccination). Differences in OT-I CD8$^+$ T cell priming were analyzed applying the Mann Whitney test, * = P < 0.05 and cytokine production by the different vaccinated groups were compared using two-way ANOVA with Bonferonni post-test, * = P < 0.05. Data shown are from one experiment using 2–4 mice per group.

isolated spleens of sensitized animals. Injected target cells were distinguished from host spleen cells by the congenic marker CD45.1. Flow cytometric analyses showed the nearly complete disappearance of the target cell population (Figure 8.6A), while this population remains present in the animals vaccinated with the non-targeted PLGA NP and still more clearly in non-vaccinated animals (Figure 8.6A). Vaccination with PLGA NP targeted to CD40, DEC205 or CD11c induced efficient *in vivo* cytotoxicity, about 80% specific killing, compared to 40% induced by non-targeted PLGA NP loaded with the same Ag and adjuvants, or no killing by the control non-vaccinated animals (Figure 8.6B).
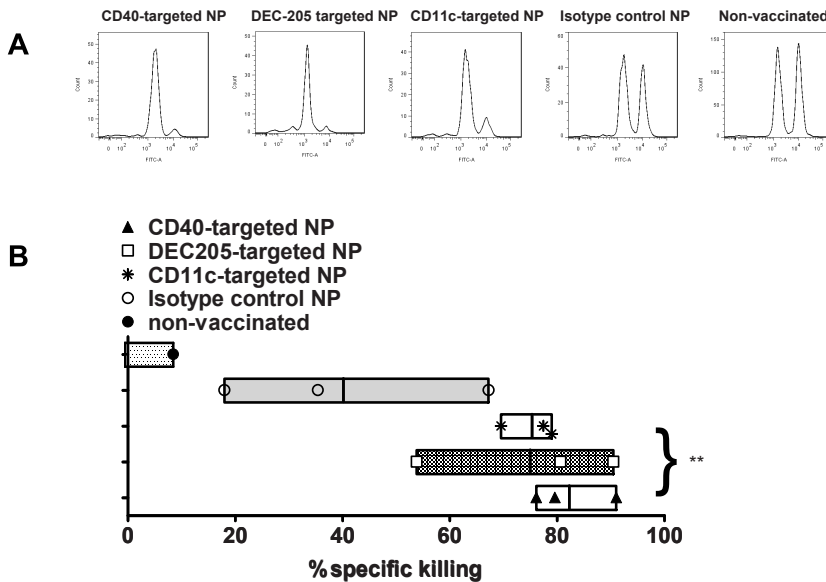

Figure 8.6   Vaccinations with PLGA-(Ag/TLR3+7L)-αCD40, DEC205 or CD11c NP induce better CD8+ T cells with potent *in vivo* cytotoxic capacity compared to PLGA-(Ag/TLR3+7L)-non-targeted NP.

C57BL/6 were vaccinated s.c. in the right flank with 10 µg OVA encapsulated in CD40, DEC-205 and CD11c- targeted PLGA-(Ag/TLR3+7L) NP or non-targeted PLGA-(Ag/TLR3+7L)-non-targeted (pull of IgG2a and IgG2b) control NP. On day 7 day post vaccination, SIINFEKL-loaded CFSE[high] OVA-specific target cells and ASNENMETM-loaded CFSE[low] INFLUENZA-specific target cells (negative controls) were injected i.v. in a 1:1 ratio. Mice were sacrificed 18 h later and the degree of OVA-specific lysis of the target cells determined by FACS (A) and the % killing of OVA-specific target cells quantified as described in M&M. *In vivo* cytotoxicity was determined using the following formula: (1-[(CFSE-peak OVA/CFSE-peak FLU)[vaccinated animals] x (CFSE-peak OVA/CFSE-peak FLU)[non-vaccinated animals]]) x 100% (B). Data shown are from one experiment consisting of 3 mice per group and differences in in vivo cytotoxicity of primed CD8+ T cells were analyzed applying an unpaired student t-test, ** = P < 0.01 comparing targeted NP versus non-targeted NP.

Discussion

Despite the large amount of successful protective vaccines against several infectious agents, efforts to develop effective therapeutic vaccines against cancer have been largely disappointing. However, effector mechanisms to eradicate cancer cells and pathogens are present in the immune system as has been demonstrated by the multiple examples of tumor immune surveillance [2,3]. Therefore, cancer vaccines should potentially be able to achieve similar success as vaccines against infectious agents [20]. However, tumors are weakly immunogenic, and therefore cancer vaccines must trigger the release of danger signals to potently activate the immune system against the tumor-associated Ags. This could be achieved by incorporating TLRLs in the vaccine formulation, which induce a strong immune response [21]. In our work we have introduced Poly I:C and R848, synthetic agonists of the TLR 3 and 7 respectively, in the PLGA NP produced in the vaccine development.

Furthermore, unless DCs are cultured and loaded *in vitro*, a technically complex and costly process, cancer vaccines could be dispersed and/or degraded in body fluids (reduced half-life) and even activate inappropriate cells when administered in soluble form via injections. Therefore, in order to protect Ags from degradation and to ensure efficient delivery of the Ag to DC, we encapsulated the model protein Ag in NP coated with polyethylene glycol (PEG), which helps to avoid non-specific interactions [22], and couple mAb targeted to CD40, DEC-205 or CD11c receptors expressed on the surface of DCs. Binding of these receptors can facilitate internalization, activation of signalling pathways which induce the maturation of DC and finally increase Ag presentation and enhance the induction of T cell responses [23-25].

The mechanism of Ag internalization by DC of targeted NP was demonstrated by the strong inhibition induced by Cytochalasin D, a potent inhibitor of actin polymerization which disrupts actin microfilaments associated with phagocytosis. Therefore, internalization of NP via CD40, DEC-205 and to a lesser extent CD11c requires actin polymerization to translocate NP towards antigen processing compartments to produce peptides for presentation by MHC class I and MHC class II. Indeed, uptake of targeted NP resulted in very efficient CD8+ and CD4+ T cell priming.

Targeting strategies to improve vaccine efficacy and to achieve increased delivery to DC have been tested by passive [26,27] and active targeting [14]. It was shown that DC targeting endocytic lectin receptors, such as DC-SIGN and DEC-205 with mAb coupled to PLGA NP induces strong CD8+ T cell responses [28,29], which demonstrated that exogenous Ags taken up by these receptors reach the cytoplasm by endosomal escape and are then presented to

8

T cells via MHC I, a process known as cross-presentation [30]. Endocytosis via CD40 has been shown to facilitate MHC class I cross-presentation of exogenous Ag by routing internalized Ag into early endosomal compartments [31] whereas DEC-205 targeted Ag are routed to late endosomes, compartments associated with sub-optimal MHC class I presentation, which was not confirmed in our work. CD11c is a receptor predominantly expressed on dendritic cells (DC), to which Ag targeting has been shown to induce an efficient Ag processing and presentation on MHC classes I and II products, as well as robust CD4$^+$ and CD8$^+$ T cell immunity [32].

In this work, although CD40 showed a trend at performing slightly better in facilitating NP uptake *in vitro*, no significant differences were observed *in vivo* between the immunological responses induced by the PLGA NP targeted to different receptors (CD40, DEC-205 or CD11c). This suggests that the most important parameter in NP vaccine targeting is to facilitate and optimize endocytic capacity of the NP by DC. The inclusion of potent TLRLs will subsequently lead to robust T cell responses, irrespective of the DC surface molecule targeted.

Therefore, the T cell priming capacity of the DC-targeted NP could be more related to the presence of TLR3 and 7 agonists than to the activation of targeted receptors itself, or at most they are additive. Possibly the activation by TLR ligands could be substantially higher than those induced by the receptors targeted by the PLGA NP, therefore hiding the effect of the latter. However, targeting seems essential, since non-targeted PLGA NP containing the TLR3 and 7 agonists did not show strong activation capacity both *in vitro* and *in vivo*. *In vivo* assays show that the PLGA NP dispersion is much higher in non-targeted NP, or at least targeting PLGA NP to phagocytic receptors seems to be important for uptake by DCs (Figure 8.5 and 6). Furthermore, the capacity to induce specific *in vivo* killing shows significant differences between targeted and non-targeted NP *in vivo* (Figure 8.6B) indicating that targeted NP can prime specific cytotoxic CD8+ T cells from the endogenous naïve T cell repertoire.

To investigate the influence of the target specificity of PLGA NP in the whole body biodistribution *in vivo*, NP were loaded with Alexa-647-OVA (fluorescent marker). 48 h post-injection mice were sacrificed and the main organs were harvested. PLGA NP can be quickly cleared from the blood by the reticulo-endothelial system or can remain in organs, such as the liver, lung and spleen, for prolonged periods of time. Design considerations, such as size, shape, surface coating and dosing, can be manipulated to prolong blood

circulation and enhance treatment efficacy, but nonspecific distribution has thus far been unavoidable. It has been described that NP remained detectable in the brain, heart, kidney, liver, lungs, and spleen after 7 days [33-35]. In our work, no obvious differences in tissue biodistribution of PLGA NP targeted to the CD11c, DEC-205 and CD40 receptors, or non-targeted (isotype control) were observed after 48 h (Supporting Information Figure S8.2). This suggests that, despite the high numbers of PLGA NP draining freely throughout the body and being available for uptake in the major organs, PLGA NP are more efficiently scavenged by DCs when carrying receptor-specific Abs. In draining lymph nodes and other lymphoid organs small differences in fluorescence intensity in favor of specific targeted NP were observed (Supporting Information Figure S8.3).

In conclusion, we present here a study using PLGA NP-vaccines containing an Ag model and TLR agonist, as adjuvants, coated with mAb targeted to specific receptors on DCs. Targeted NP have shown to be a potent system to induce strong immune responses, both CD4 and CD8 *in vitro* and *in vivo*. Due to the flexibility of the PLGA to encapsulate multiple polypeptide Ags, this is a versatile system to develop NP-vaccines tailored to different types of tumors.

Acknowledgements

8

References

1.   Dunn GP, Bruce AT, Ikeda H, Old LJ, Schreiber RD 2002. Cancer immunoediting: from immunosurveillance to tumor escape. Nature immunology 3(11):991-998.

2.   Swann JB, Smyth MJ 2007. Immune surveillance of tumors. The Journal of clinical investigation 117(5):1137-1146.

3.   Kim R, Emi M, Tanabe K 2007. Cancer immunoediting from immune surveillance to immune escape. Immunology 121(1):1-14.

4.   Hutchings CL, Gilbert SC, Hill AV, Moore AC 2005. Novel protein and poxvirus-based vaccine combinations for simultaneous induction of humoral and cell-mediated immunity. Journal of immunology 175(1):599-606.

5.   Paschen A, Eichmuller S, Schadendorf D 2004. Identification of tumor antigens and T-cell epitopes, and its clinical application. Cancer immunology, immunotherapy : CII 53(3):196-203.

6.   Spagnoli GC, Adamina M, Bolli M, Weber WP, Zajac P, Marti W, Oertli D, Heberer M, Harder F 2005. Active antigen-specific immunotherapy of melanoma: from basic science to clinical investigation. World journal of surgery 29(6):692-699.

7.   Banchereau J, Briere F, Caux C, Davoust J, Lebecque S, Liu YJ, Pulendran B, Palucka K 2000. Immunobiology of dendritic cells. Annu Rev Immunol 18:767-811.

8.   Celluzzi CM, Mayordomo JI, Storkus WJ, Lotze MT, Falo LD, Jr. 1996. Peptide-pulsed dendritic cells induce antigen-specific CTL-mediated protective tumor immunity. The Journal of experimental medicine 183(1):283-287.

9.   Steinman RM 1991. The dendritic cell system and its role in immunogenicity. Annual review of immunology 9:271-296.

10.   Delamarre L, Mellman I 2011. Harnessing dendritic cells for immunotherapy. Seminars in immunology 23(1):2-11.

11.   Blander JM, Medzhitov R 2006. Toll-dependent selection of microbial antigens for presentation by dendritic cells. Nature 440(7085):808-812.

12.   Schlosser E, Mueller M, Fischer S, Basta S, Busch DH, Gander B, Groettrup M 2008. TLR ligands and antigen need to be coencapsulated into the same biodegradable microsphere for the generation of potent cytotoxic T lymphocyte responses. Vaccine 26(13):1626-1637.

13.   Wille-Reece U, Flynn BJ, Lore K, Koup RA, Kedl RM, Mattapallil JJ, Weiss WR, Roederer M, Seder RA 2005. HIV Gag protein conjugated to a Toll-like receptor 7/8 agonist improves the magnitude and quality of Th1 and CD8+ T cell responses in nonhuman primates. Proceedings of the National Academy of Sciences of the United States of America 102(42):15190-15194.

14.   Tacken PJ, de Vries IJ, Torensma R, Figdor CG 2007. Dendritic-cell immunotherapy: from ex vivo loading to in vivo targeting. Nat Rev Immunol 7(10):790-802.

15.   Rolink A, Melchers F, Andersson J 1996. The SCID but not the RAG-2 gene product is required for S mu-S epsilon heavy chain class switching. Immunity 5(4):319-330.

16. Cruz LJ, Tacken PJ, Rueda F, Domingo JC, Albericio F, Figdor CG 2012. Targeting nanoparticles to dendritic cells for immunotherapy. Methods in enzymology 509:143-163.

17. Cruz LJ, Tacken PJ, Bonetto F, Buschow SI, Croes HJ, Wijers M, de Vries IJ, Figdor CG 2011. Multimodal imaging of nanovaccine carriers targeted to human dendritic cells. Molecular pharmaceutics 8(2):520-531.

18. Rosalia RA, Quakkelaar ED, Redeker A, Khan S, Camps M, Drijfhout JW, Silva AL, Jiskoot W, van Hall T, van Veelen PA, Janssen G, Franken K, Cruz LJ, Tromp A, Oostendorp J, van der Burg SH, Ossendorp F, Melief CJ 2013. Dendritic cells process synthetic long peptides better than whole protein, improving antigen presentation and T-cell activation. European journal of immunology 43(10):2554-2565.

19. Moore MW, Carbone FR, Bevan MJ 1988. Introduction of soluble protein into the class I pathway of antigen processing and presentation. Cell 54(6):777-785.

20. Umar A, Dunn BK, Greenwald P 2012. Future directions in cancer prevention. Nature reviews Cancer 12(12):835-848.

21. Heine H, Lien E 2003. Toll-like receptors and their function in innate and adaptive immunity. International archives of allergy and immunology 130(3):180-192.

22. Cruz LJ, Tacken PJ, Fokkink R, Joosten B, Stuart MC, Albericio F, Torensma R, Figdor CG Targeted PLGA nano- but not microparticles specifically deliver antigen to human dendritic cells via DC-SIGN in vitro. J Control Release 144(2):118-126.

23. Geijtenbeek TB, Gringhuis SI 2009. Signalling through C-type lectin receptors: shaping immune responses. Nature reviews Immunology 9(7):465-479.

24. Elgueta R, Benson MJ, de Vries VC, Wasiuk A, Guo Y, Noelle RJ 2009. Molecular mechanism and function of CD40/CD40L engagement in the immune system. Immunological reviews 229(1):152-172.

25. Figdor CG, van Kooyk Y, Adema GJ 2002. C-type lectin receptors on dendritic cells and Langerhans cells. Nature reviews Immunology 2(2):77-84.

26. Zhang Z, Tongchusak S, Mizukami Y, Kang YJ, Ioji T, Touma M, Reinhold B, Keskin DB, Reinherz EL, Sasada T 2011. Induction of anti-tumor cytotoxic T cell responses through PLGA-nanoparticle mediated antigen delivery. Biomaterials 32(14):3666-3678.

27. Manolova V, Flace A, Bauer M, Schwarz K, Saudan P, Bachmann MF 2008. Nanoparticles target distinct dendritic cell populations according to their size. European journal of immunology 38(5):1404-1413.

28. Raghuwanshi D, Mishra V, Suresh MR, Kaur K 2012. A simple approach for enhanced immune response using engineered dendritic cell targeted nanoparticles. Vaccine 30(50):7292-7299.

29. Tacken PJ, Figdor CG 2011. Targeted antigen delivery and activation of dendritic cells in vivo: steps towards cost effective vaccines. Seminars in immunology 23(1):12-20.

30. Burgdorf S, Kurts C 2008. Endocytosis mechanisms and the cell biology of antigen presentation. Current opinion in immunology 20(1):89-95.

8

31. Chatterjee B, Smed-Sorensen A, Cohn L, Chalouni C, Vandlen R, Lee BC, Widger J, Keler T, Delamarre L, Mellman I 2012. Internalization and endosomal degradation of receptor-bound antigens regulate the efficiency of cross presentation by human dendritic cells. Blood 120(10):2011-2020.

32. Castro FV, Tutt AL, White AL, Teeling JL, James S, French RR, Glennie MJ 2008. CD11c provides an effective immunotarget for the generation of both CD4 and CD8 T cell responses. European journal of immunology 38(8):2263-2273.

33. Almeida JP, Chen AL, Foster A, Drezek R 2011. In vivo biodistribution of nanoparticles. Nanomedicine 6(5):815-835.

34. Sa LT, Albernaz Mde S, Patricio BF, Falcao MV, Jr., Coelho BF, Bordim A, Almeida JC, Santos-Oliveira R 2012. Biodistribution of nanoparticles: initial considerations. Journal of pharmaceutical and biomedical analysis 70:602-604.

35. Semete B, Booysen L, Lemmer Y, Kalombo L, Katata L, Verschoor J, Swai HS 2010. In vivo evaluation of the biodistribution and safety of PLGA nanoparticles as drug delivery systems. Nanomedicine 6(5):662-671.

Supporting Information

Analysis of PLGA NP kinetic uptake by DC *in vitro*

DCs from wild type C57BL/6 mice were incubated with different PLGA NP (CW800-Ag/TLR3+7L)- targeted to CD40, DEC205 and CD11c receptors and isotype control (non-targeted) respectively at 37°C to determine their kinetic of internalization capacity towards DCs (Supporting Information Figure S8.1). Thereby, the kinetics uptake was studied during 24 h. Fluorescence intensity was measured by odyssey scanning by the ratio of PLGA NP containing CW800-OVA at 800 nm and the number of cell amount determined by nuclei staining at 700 nm. The ratio value indicates the level of uptake of PLGA NP to DC. A direct relation between the PLGA NP concentration and uptake capacity was observed. Targeted PLGA NP showed statistically significant differences with respect to their non-targeted counterparts.
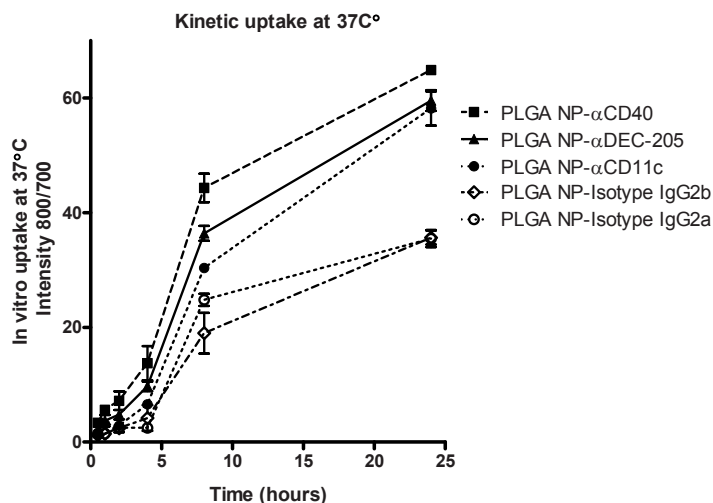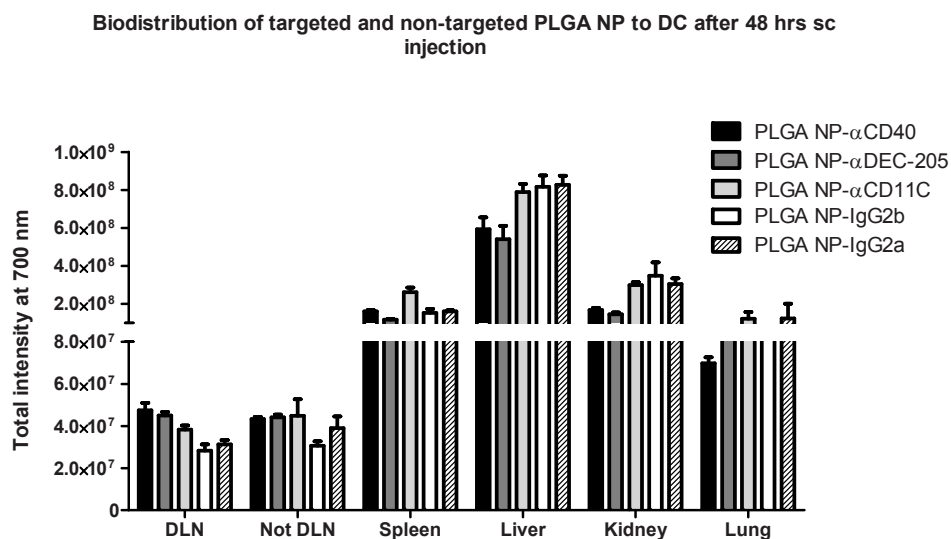

Supporting Information Figure S8.1   Kinetic uptake of targeting NP to DC improves internalization compared to non-targeted NP.
WT C57BL/6 BMDC (100000 cells/well) were incubated with fixed amounts of 5 µg/mL PLGA-(Ag/TLR3+7L)-αCD40, PLGA-(Ag/TLR3+7L)-αDEC-205 and PLGA-(Ag/TLR3+7L)-αCD11c NP or isotype control (PLGA-(Ag/TLR3+7L)-IgG2a and PLGA-(Ag/TLR3+7L)-IgG2b) NP-formulations at distinct time points at 37°C. Following washing for the removal of unbound PLGA NP cells were co-stained with DNA-binding TO-PRO®, allowing quantification of number of cells per well and correlation with PLGA NP-binding or uptake per cells. Fluorescence intensity was measured by scanning on the Odyssey (Li-Cor) and results show the ratio of 800/700 nm fluorescence intensities of a duplicate analysis + deviation. Data are from one out of two independent experiments performed with two different batches of PLGA NP.

8

Biodistribution of targeted and non-targeted PLGA NP

No obvious differences in tissue biodistribution of PLGA NPs targeted to the CD11c, DEC-205 and CD40 receptors, or non-targeted (isotype control) were observed after 48 h (Supporting Information Figure S8.2). This suggests that, despite the fact that high numbers of PLGA NPs drain freely throughout the body and are available for uptake, PLGA NP are more efficiently scavenged by DCs when carrying receptor-specific Abs. Although PLGA NP were mainly found in major organs of the body as previously described, in draining lymph nodes (DLN) and other lymphoid organs differences in fluorescence intensity in favor of specific targeted NP were observed.

Biodistribution of targeted and non-targeted PLGA NP to DC after 48 hrs sc injection

Supporting Information Figure S8.2   Biodistribution of targeting and non-targeted PLGA NP. Mice were vaccinated s.c. with 10 µg of Alexa-647-OVA. Mice were sacrificed 48 h post-injection and the main organs were harvested. Tissue biodistribution profile of targeted and non-targeted PLGA NPs harboring Alexa-647-OVA was determined. Relative fluorescent values were determined for each group depicted as mean ± SEM (D).

Better *in vivo* DC-uptake of targeted PLGA-(Ag/TLR3+7L) NP compared to non-targeted PLGA NP

This suggests that high numbers of PLGA NPs are specifically taken up by DCs in the spleen. Therefore, PLGA NP are more efficiently scavenged by DCs when carrying receptor-specific Abs (Supporting Information Figure S8.3).
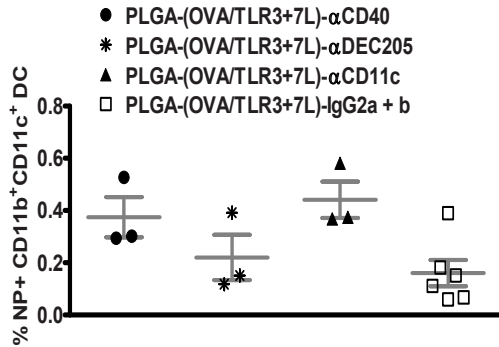
Supporting Information Figure S8.3   Improved *in vivo* DC-uptake by targeted PLGA-(Ag/TLR3+7L) NP compared to isotype control and non-targeted PLGA NP.
C57BL/6 animals were vaccinated s.c. in the right flank with 10 µg OVA-Alexa647 encapsulated in PLGA-(Ag/TLR3+7L)-αCD40, PLGA-(Ag/TLR3+7L)-αDEC-205 or PLGA-(Ag/TLR3+7L)-αCD11c NP, as well as with non-targeted PLGA-(Ag/TLR3+7L)-IgG2a and PLGA-(Ag/TLR3+7L)-IgG2b NP. Animals were sacrificed 48 hr post-vaccination and the Spleen harvested and single-cell suspensions prepared. Analysis by flow cytometry of the different immune cell populations which were positive for Alexa-647 fluorescence was performed by staining cells with various fluorescent antibodies. Results shown are from one experiment using 3 mice per group.

8